Experimental data show a significant reduction in test application time for most of the circuits, an average of 36% with two peak gains of 66%. It can also be noted that, as the number of memory elements increase, the improvement for removing a scan-in set operation step up. Thus, the interleaved scan is expected to scale well with design complexity.

Few benchmarks, like s635 and s641, are so *hard-to-test* that almost all ATPG-generated full-scan vectors are required in the interleaved-scan test pattern, thus, gain is strongly limited. On the other hand, benchmark s9234 deserves special consideration and is currently under study.

5. Conclusions

Interleaved scan is a promising test architecture for reducing the number of clock cycles required for a test session. Interleaved scan requires an effective optimisation algorithm to extend the test vectors generated by a standard ATPG. A local-search technique has been presented to address this issue, based on explicit neighborhood exploration and exploiting the concept of population. A prototype was

tested on the standard ISCAS benchmarks and the experimental results show the effectiveness of the proposed approach. Authors are experimenting the interleaved scan on a larger set of circuits to better assess its applicability. Simultaneously, they are working on applying the evolutionary core proposed in this paper to different problems.

1. *Bushnell M.L., Agrawall V.D. Essentials of Electronic Testing forDigital, Memory & Mixed Signals VLSI Circuits, Kluwer Academic Publishing, 2000.*

2. *Niermann T.M., Roy R.K., Pasel J.H., Abraham J.A. Test Compaction for Sequential Circuits // IEEE Transactions on Computer-Aided Design, February 1992, pp. 260–267.*

3. *Pomerantz I., Reddy L N., Reddy S.M. COMPACTEST: A Method to Generate Compact Test Sets for Combinational Circuits // IEEE Transactions on Computer-Aided Design, November 1993, pp. 1361-1371.*

4. *Brglez F., D. Bryant, Kozminski K. Combinational profiles of sequential benchmark circuits // Proc. Int. Symp. on Circuits And Systems, 1989, pp. 1929-1934.*

5. *Goldberg E. Genetic Algorithms in Search, Optimization, and Machine Learning // Addison-Wesley, 1989.*

I. Bolshakova[1], V. Brudnyi[2], N. Kolin[3], P. Koptsev[1], Ya. Kost[1], N. Kovaleva[1], O. Makido[1], T. Moskovets[1], F. Shoorigin[1]

[1] Lviv Polytechnic National University, Lviv, Ukraine,

[2] Siberian Physical Technical Institute, Tomsk, Russia,

[3] Obninsk Branch State Research Center “Karpov Institute of Physical Chemistry”, Obninsk, Russia

THE BEHAVIOUR OF InSb UNDER THE IRRADIATION WITH REACTOR NEUTRONS

In the paper, is investigated the influence of the irradiation with full reactor neutron spectrum up to the fluence of $F=3\cdot10^{16}$ cm^{-2} upon the electrophysical properties of complex doped InSb microcrystals and thin film InSb samples with charge carrier concentration of $n=(9\cdot10^{16}\div3\cdot10^{18})$ cm^{-3}. The influence of the initial doping level on the radiation resistance is determined. The optimal charge carrier concentration for the manufacturing of the radiation resistant magnetic field microsensors is determined and is equal to $n=(6\div7)\cdot10^{17}$ cm^{-3} for the complex doped InSb microcrystals, and $n=3\cdot10^{17}$ cm^{-3} for thin film samples.

Introduction

The InSb semiconductor material, owing to its electrophysical properties (high charge carrier mobility, performance etc) has found its practical application as a sensitive element in magnetic field sensors, intended for operation in extreme conditions.

The feature of the presented experiment is that the InSb samples investigation was performed directly under their irradiation with full neutron flux in the Fast Pulsed Reactor (IBR-2) reactor channel in Joint Institute of Nuclear Research (Dubna, Russia). The change of electrophysical parameters of the samples with accuracy of 0.01% was measured directly under the irradiation, which allowed obtaining the sufficient information volume, which is very important for the understanding of the processes occurring in the semiconductor material under the high energy particles influence. Besides, the data of the strongly doped InSb samples irradiation with neutrons of different energies are practically absent in the literature and the results presented in the paper are filling this gap.

The Experiment

The study of the influence of the irradiation with full reactor neutrons spectrum was performed on the InSb semiconductor microcrystals and thin film samples with different doping level. The InSb microcrystals have been grown from gas phase by the Chemical Transport Reaction method, which allows achieving the material with sufficiently high structural perfection. During the growth process they were doped with impurity complex, that includes Sn, Al, and Cr. Thin film samples of InSb/i-GaAs heterostructure were obtained by the molecular-beam deposition.

The major nuclear reactions of the indium and stibium with thermal and intermediate neutrons, present in the reactor neutron flux, are the reaction of the type as follows [3]:

$$^{113}In(n,\gamma),\ ^{114}In \underset{49 days}{\overset{\beta}{\rightarrow}} {}^{114}Sn$$

$$^{115}In(n,\gamma),\ ^{116}In \underset{54\,\mathrm{min}}{\overset{\beta}{\rightarrow}} {}^{116}Sn$$

$$^{121}Sb(n,\gamma),\ ^{122}Sb \underset{2,8 days}{\overset{\beta,\gamma}{\rightarrow}} {}^{122}Te$$

$$^{123}Sb(n,\gamma),\ ^{124}Sb \underset{21 days}{\overset{\beta,\gamma}{\rightarrow}} {}^{124}Te$$

In this case the nuclear reaction products concentration depends on the value of thetrmal capture cross-section by the basic atoms of semiconductor compound. The thermal cross-section by the indium atoms is 190 barn, and for the stibium atoms it is 5.5 barns. Therefore, during the transaction of such nuclear reactions the stannum is the major (97.5%) end product, and the Te isotopes does not exceed 2%.

So, taking it into the consideration, the major doping impurity for the given impurity complex that provides the necessary doping level Sn has been chosen. The Al and Cr impurities was introduced for the improvement of the material characteristics stability.

The dimensions of the InSb microcrystalline samples prepared for the investigation was 0,7×0,07×0,03 mm^3, and the dimensions of sensitive element of the InSb/i-GaAs thin film samples was 0,4×0,3×0,002 mm^3. The main parameters of the sensors under the investigation (at T=300K): initial charge carrier concentration $n=(9\cdot10^{16}\div3\cdot10^{17})$ cm^{-3}; the charge carrier mobility $\mu=(5,2\div1,0)\cdot10^4$, $cm^2\cdot V^{-1}\cdot s^{-1}$; the resistance $\rho=(14,3\div2,1)\cdot10^{-4}$, Ohm·cm.

As a result of the performed experiment the InSb microcrystal samples and InSb/i-GaAs heterostructures have been irradiated by the reactor neutrons with average energy of E=1.5 MeV with average flux intensity of $j= 9\cdot10^9$ $cm^{-2}\cdot s^{-1}$ up to the fluence of $F=3\cdot10^{16}$ cm^{-2}. The du ration of the irradiation is 996 hours.

Results and discussion

The experimental results of the relative charge carrier concentration change measurement $\left(\frac{\Delta n}{n}\right)$ vs neutron fluence (F_N) is presented in table 1 and in Fig. 1.

Table 1

The relative InSb charge carrier concentration change (Δn/n, %) vs obtained radiation dose

#	Initial charge carrier concentration n, cm^{-3}	Relative charge carrier concentration change Δn/n, %			
		Session duration, hrs	**40,5**	**300**	**560**	**996**
		Neutron fluences F, cm^{-2}	**$1{,}0\cdot10^{15}$**	**$7{,}4\cdot10^{15}$**	**$1{,}7\cdot10^{16}$**	**$3{,}0\cdot10^{16}$**
InSb microcrystals						
1	$8{,}6\cdot10^{16}$		1,62	9,3	16,1	24,0
2	$6{,}4\cdot10^{17}$		0,04	0,6	0,9	0,8
3	$9{,}7\cdot10^{17}$		-0,05	-0,4	-1,2	-3,3
Thin film InSb/i-GaAs samples						
4	$3{,}0\cdot10^{18}$		-0,3	-2,0	-4,3	-8,2
5	$7{,}5\cdot10^{17}$		-0,5	-2,2	-4,3	-7,3
6	$3{,}3\cdot10^{17}$		-0,5	-1,1	-2,3	-4,5

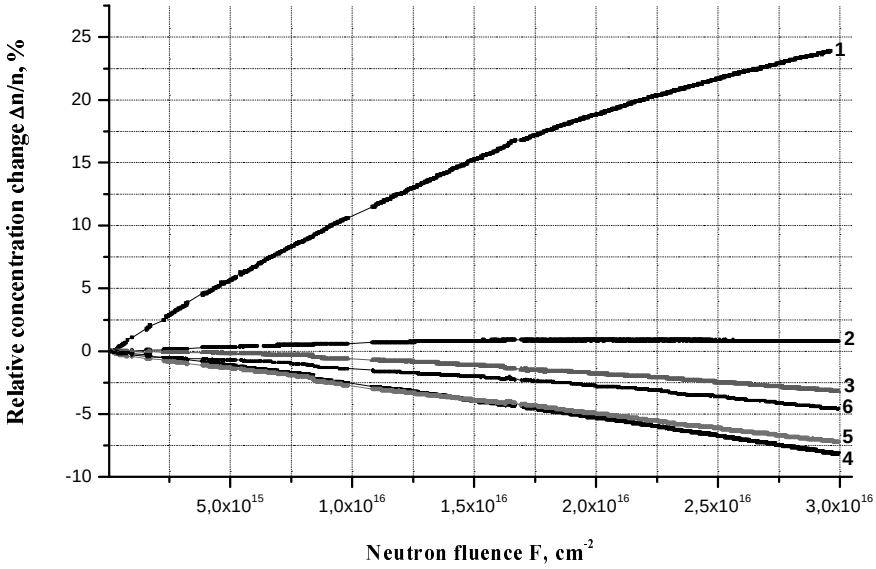

Fig. 1. The dose dependence of the relative charge carrier concentration change (curve number coincides with the number of sample in Table 1)

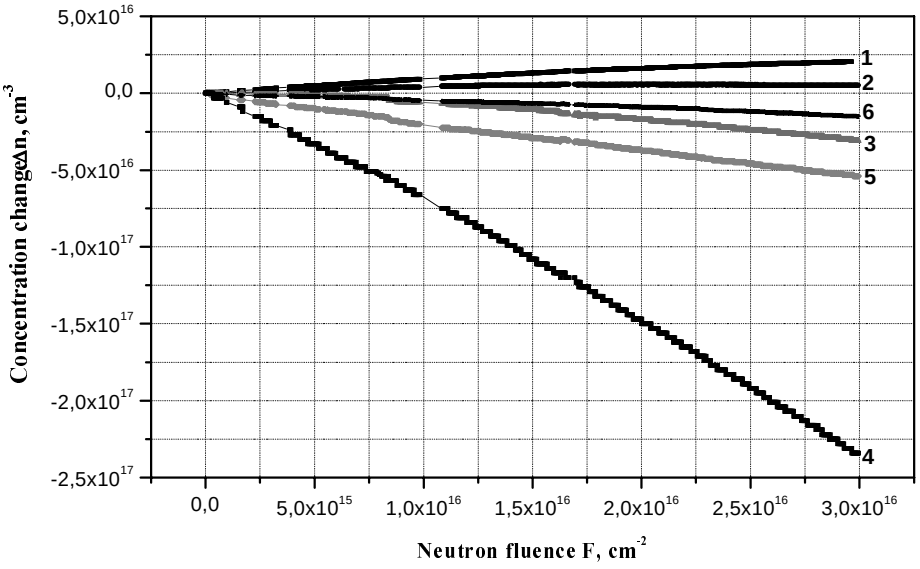

Fig. 2. Dose dependence of absolute charge carrier concentration change (the number of the curve coincides with sample number in table 1)

As the results have shown, in the investigated reactor neutron fluence range almost linear charge carrier concentration change is observed. In this case, the behavior of the microcrystals depends on the charge carriers initial concentration, i.e. on the initial doping level of the material. In case of small values of the charge carrier concentration in microcrystals (sample 1, n_{in}=8.6·10^{16} cm^{-3}) the charge carrier concentration growth is observed while reactor neutron fluence increasing. For the sample 2 (initial charge carrier concentration n_{in}=6,4·10^{17} cm^{-3}) the charge carrier concentration change is practically not observed up to the fluence of 3·10^{16} cm^{-2}. In case of further growth of the initial concentration the change of the sign of the relative concentration change is observed. For the sample 3 (n_{il}=9,7·10^{17} cm^{-3}) in case of increasing of the neutron fluence the decreasing of the charge carrier concentration in the material is observed. The behavior of the microcrystalline sensors proves the investigations on radiation resistance of the InSb microcrystals under the irradiation with reactor neutrons performed before, in particular the dependence of relative charge carrier concentration change under the irradiation vs initial charge carrier concentration, i.e. vs the amount of doping impurity and type of its introducing into the crystalline lattice of the material.

In microsensors, manufactured on the base of epitaxial films (samples 4-6) the charge carrier concentration in irradiated samples decreases, while the initial charge carrier concentration in initial material and the neutron fluence increases, moreover, the higher n_{in} is, the higher is the charge carrier concentration decreasing velocity in the material.

The dependencies of charge carrier change velocity ($\frac{\Delta n}{\Delta F_f}$) in irradiated samples vs charge carrier concentration in initial material for microcrystals (samples 1-3) and epitaxial films (samples 4-6) are given in Fig. 3. The charge carrier concentration change velocity is given for the maximal reactor neutron fluence of 3·10^{16} cm^{-2}. The data for the microcrystals with different initial charge carrier concentration after the irradiation with a reactor neutron fluence of 1,7·10^{15} cm^{-2} is also given for the comparison.

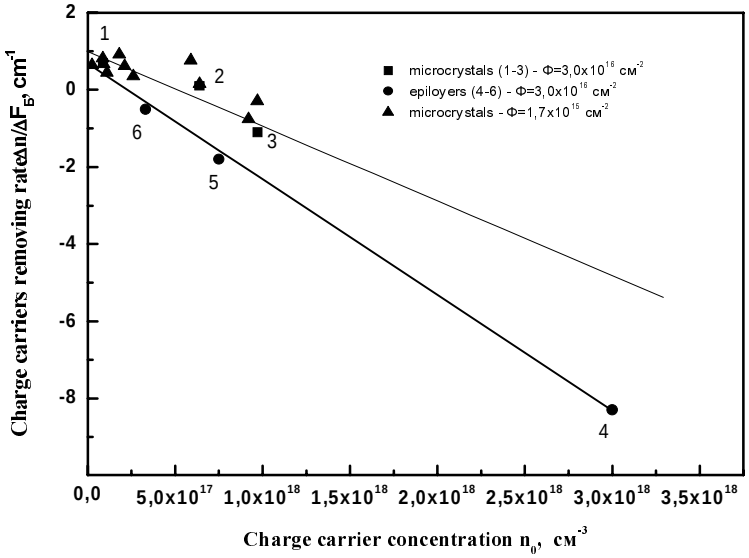

Fig. 3. The concentration dependence of the charge carrier removal under the neutron irradiation up to the fluence of F=3·10^{16} cm^{-2} (the sample number coincides with the sample number in Table 1).

As one may see from the Fig. 3. for the epitaxial layers (sample 4-6) almost linear dependencies of the charge carrier removal velocity vs charge carrier concentration in initial material are observed. For the microcrystals the increasing of the charge carrier exhaust velocity is observed while the charge carrier concentration in initial material increases. However, under the irradiation with the neutrons in IBR-2 reactor of sample 2, the charge carrier concentration practically does not change within the whole fluence range under the investigation (see Table 1.). This manifests that among the samples under the investigation in case of irradiation in stated conditions the sample 2 has the highest radiation resistance.

The difference of the InSb microcrystals and epitaxial films behavior during this experiment, obviously, may be explained by the peculiarities of radiation defect creation in samples of different thickness and structural perfection.

For the numerical explanation of the radiation-physical processes occurring in the InSb under the irradiation with reactor neutrons, it is necessary to take into consideration two major factors of radiation defects creation in the material under the influence of fast neutrons, recoil atoms and gamma-component of the reactor irradiation and doping atoms creation due to the nuclear reactions, occurring during the interaction of thermal and intermediate neutrons with atoms of the base material.

It is known [5], the creation of Sn atoms under the irradiation depends only on the value of neutron fluence and does not depend on charge carrier concentration in the initial material. From the result analysis (Fig. 3) one may see that in the neutron fluence range under the investigation the charge carrier concentration change velocity may be presented by the linear dependence as follows:

$$\left(\frac{\Delta n}{\Delta F_n}\right) = \alpha - \beta \cdot \left(n_0 + \alpha \cdot F_f - n_i(300K)\right),$$

where α - the coefficient which describes the introduction of stannum atoms (cm^{-1}); β - acceptor type defect creation intersection (cm^2); $n_i(300K) = 2 \cdot 10^{16}$ cm^{-3} – intrinsic electron concentration in InSb at 300K.

The results obtained earlier [5] on irradiation of InSb samples with high fluences of full reactor neutrons spectrum for nuclear doping performance are the evidence that the major part of the impurity introduced into the material (in this case of the Sn) is in electrically active state right after the irradiation (without further thermal treatment). This will determine the major electrophysical characteristics of the irradiated samples. The decreasing, in that way, of the introduced Sn due to the cut off slow neutrons in flux (irradiation in Cd-box [6]) causes the major electrophysical parameters of the irradiated samples are determining only by the created radiation defects (RD). Separate determination of the RD contribution, created during the irradiation, and introduced Sn impurity onto the irradiated InSb samples with different initial charge carrier concentration is one of the primary tasks, which solution will allow explaining of the radiation-physical processes, occurring in the materials.

The performed calculations of the slow and intermediate neutron flux density in neutron spectrum of the IBR-2 pulsed reactor allowed the determination of their values in total neutron flux, that are correspondently equal to 20% and 25% from the integral fast neutron flux.

Besides, for the In atoms there is resonance neutron adsorption ($\sigma_0 \approx 4 \cdot 10^4$ barn) with energy of 1.46 eV, which flux density in InSb decreases by e times on depth of the order of 10 μm [5]. Taking into consideration the small dimensions of the microcrystals and epitaxial films during the calculation of the introduced Sn one should take into account also the contribution of the resonance neutrons.

For the given neutron spectrum the concentration of stannum impurity, that is introduced as a result of the nuclear reactions on In atoms, was calculated [7]. The obtained value of Sn introducing factor on thermal neutrons is equal to 0,56 cm^{-1}, on the intermediate neutrons taking into account the maximum resonance – 0.19 cm^{-1}, ant total value of the Sn introducing factor α=0,75 cm^{-1} (the factor is normalized for one fast neutron).

The stated value of α coincides with charge carrier change velocity in low-doped sample 1 with sufficient accuracy. It is equal for all samples and therefore it may be deducted from the experimental values $\frac{\Delta n}{\Delta F_n}$. Then in fig. 3 the line of concentration dependence $\frac{\Delta n}{\Delta F_n} = f(\mathrm{n_{вих}})$ will cross the point of origin.

In the dependence $\frac{\Delta n}{\Delta F_n} = f(\mathrm{n_{вих}})$ in case of certain initial charge carrier concentration the value of charge carrier removal velocity $\frac{\Delta n}{\Delta F_n}$=0. One may conclude, that namely the additional doping by stannum during the irradiation with full reactor neutron spectrum causes this situation, and the specific concentration

$n(\frac{\Delta n}{\Delta F_n}=0)$ for the given material depends on the reactor neutron spectrum in the irradiation area. Small changes of n during the irradiation are extremely important for the construction of stable Hall sensors.

Conclusions

The relative charge carrier concentration change occurs under the influence of irradiation with reactor neutrons by two mechanisms: by means of nuclear doping under the influence of thermal and resonance neutrons and on account of creation radiation defects in the material of mostly acceptor type.

The obtained results are indicating that during the irradiation of IBR-2 reactor neutrons up to the fluence of the order of $3\cdot10^{16}$ cm^{-2} the most resistant to the irradiation influence are InSb microcrystalline samples with initial charge carrier concentration of the order of $(6\div7)\cdot10^{17}$ cm^{-3} and epitaxial film samples with $n_o\approx 3\cdot10^{17}$ cm^{-3}, which may be considered as a major recommendation during the selection of the material for magnetic field radiation resistant microsensors manufacturing. In case of irradiation with neutrons with different energy spectrum, the value of the optimal charge carrier concentration in initial material will change by means of different Sn atoms introducing, that are introduced as a result of nuclear reactions on thermal and intermediate neutrons.

In case of reactor neutron fluence of $3\cdot10^{16}$ cm^{-2} the relative charge carrier concentration change in microcrystals (sample 2) does not exceed 1%, and in epitaxial films (sample 6) it does not exceed 5%. At the same time for the ordinary bulk InSb crystals the similar changes are observed at considerably lower neutron fluence $\approx 1\cdot10^{15}$ cm^{-2} [6].

1. Bolshakova I. Improvement of radiation resistance of magnetic field microsensors // Sensors & Actuators: A. Physical. – 1999. – Vol.76. – P.152-155.

2. Кудриани Н.И. Отжиг радиационных дефектов и подвижность электронов в антимониде индия, облученном быстрыми нейтронами // Фізика и техника полупроводников, 1969, т. 3, в.11 – с.1189-1192.

3. Колин Н.Г. Ядерное легирование и радиационное модифицирование полупроводников: состояние и перспективы // Известия ВУЗов. Физика. 2003, т.45, в.6 – с.12-20.

4. F. Terra, G. Fakhim, I.A. Bol'shakova, S. Leroi, E.Yu. Makido, A. Matkovskii, and T. Moskovets Fabrication, investigation, and application of doped indium antimonide microcrystals in radiation resistant sensors // Russian Physics Journal. – 2003. – Vol.46, №6. – P.601-608.

5. Н.Г.Колин, Д.И.Меркурисов, С.П.Соловьев. Электрофизические свойства ядерно-легированного антимонида индия // Физика и техника полупроводников, 1999, т. 33, в.7 – с.774-777.

6. Колин Н.Г., Меркурисов Д.И., Соловьев С.П. Электрофизические свойства InSb, облученного быстрыми нейтронами реактора // Физика и техника полупроводников, 1999, т. 33, в.8, – с. 927-930.

7. К. Бекурц, К. Виртц. Нейтронная физика. – М.: Атомиздат, 1968 г., – 456 с.